Available online at www.sciencedirect.com
ScienceDirect
Journal of Power Sources 172 (2007) 908–912
JOURNAL OF POWER SOURCES
www.elsevier.com/locate/jpowsour

Short communication

Electrochemical properties of tin phosphates with various mesopore ratios

Joon-Gon Lee, Dongyeon Son, Chunjoong Kim, Byungwoo Park *

Department of Materials Science and Engineering, and Research Center for Energy Conversion and Storage, Seoul National University, Seoul 151-744, Republic of Korea

Received 12 April 2007; received in revised form 12 June 2007; accepted 12 July 2007
Available online 2 August 2007

Abstract

Tin phosphates with various mesopore ratios are synthesized with surfactants as templates. The mesopore ratios of the tin phosphates are controlled by adjusting the surfactant: inorganic precursor ratios. As an anode material for Li-ion batteries, the mesoporous and non-mesoporous mixture with a high mesopore ratio exhibits enhanced cycling stability. Compared with the ~34% (~135 mAh g^{-1}) capacity retention after 50 cycles of the non-mesoporous tin phosphate (between 2.5 and 0.001 V), the tin-phosphate anodes with mesopore ratios of 42, 82 and 100% show capacity retentions that are enhanced by more than 50%, showing charge capacities of ~260, ~290, and ~325 mAh g^{-1}, respectively (after 50 cycles). The mesoporous structures may alleviate the large volume change of the Sn nanoparticles embedded in the lithium-phosphate matrix during charge–discharge. Cycling tests of the 100% mesoporous tin phosphate between 0.8 and 0.001 V exhibit no capacity decay: ~325 mAh g^{-1} remains after 50 cycles. This is probably because re-oxidation of metallic tin with lithium-phosphate matrix does not occur.

Keywords: Energy storage; Electrochemical properties; Mesopore; Lithium-ion battery; Tin phosphate; Capacity retention

1. Introduction

The development of portable electronics and hybrid electric vehicles (HEVs) requires Li-ion batteries with high specific energy. Although commercially used graphite anodes have good electrochemical properties, their capacity (372 mAh g^{-1} for LiC_6) is insufficient to satisfy the market requirements. Thus, tin-based anode materials such as metallic tin [1,2], tin oxides [3–5], and tin phosphates [6,7] have attracted much attention. Their theoretical capacities are two- or three-times larger (metallic tin: 959 mAh g^{-1}, SnO_2: 781 mAh g^{-1} and $Sn_2P_2O_7$: 572 mAh g^{-1}, all for $Li_{4.4}Sn$) than that of graphite anodes. They have poor capacity retention however, due to their large volume change of over 300% during lithiation/delithiation. To enhance their capacity retention, mesoporous structures [8,9], which are generally synthesized using surfactants as templates and have pore sizes between 2 and 50 nm, have been applied to these tin-based materials [10–14].

The mesoporous structures of tin-based materials may act as buffer structures to alleviate the large volume change. Though tin-phosphate materials that consist of mesoporous and non-mesoporous composites have previously been studied [12–14], the effects of the mesopore ratio on their electrochemical properties remain unclear. In this study, tin phosphates with various mesopore ratios are synthesized, and their electrochemical properties examined.

2. Experimental

Tin phosphates with various mesopore ratios were prepared by mixing various amounts of SnF_2 and H_3PO_4, and dissolving them in 40 ml of distilled–deionized water. Then, 5.5 g of cetyl-trimethyl-ammonium bromide (CTAB: $CH_3(CH_2)_{15}N(CH_3)_3Br$) was dissolved in 20 ml of distilled–deionized water, and this solution was added to the SnF_2/H_3PO_4 solution. The molar ratio of SnF_2/H_3PO_4 was fixed at 1.35, while CTAB/H_3PO_4 molar ratios of 0.11, 0.22, 0.54 and 1.10 were prepared. The mixture was stirred at 40 °C for 1 h, loaded in an autoclave, and then kept at 90 °C for 24 h. After cooling to room temperature, the precipitates

* Corresponding author. Tel.: +82 2 880 8319; fax: +82 2 885 9671.
E-mail address: byungwoo@snu.ac.kr (B. Park).

0378-7753/$ – see front matter © 2007 Elsevier B.V. All rights reserved.
doi:10.1016/j.jpowsour.2007.07.051

Table 1
Mesostructural characteristics of as-synthesized tin phosphates with various mesopore ratios

$CTAB/H_3PO_4$ precursor molar ratio	Mesopore d spacing (nm)	Average pore size (nm)	BET surface area ($m^2\ g^{-1}$)	Relative mesopore ratio (%)	Composition of synthesized Sn-P-O
0.11	–	–	14.7	0	$Sn_{1.94}P_2O_{7.3}$
0.22	4.29 ± 1.21	2.56	114	42	$Sn_{2.30}P_2O_{7.5}$
0.54	4.34 ± 0.68	2.32	167	82	$Sn_{2.61}P_2O_{7.8}$
1.10	4.20 ± 0.63	2.33	221	100	$Sn_{2.77}P_2O_{8.1}$

were recovered by centrifugal filtration, washed with distilled water and ethanol, and vacuum-dried at 100 °C for 10 h. The as-prepared powders were then annealed at 400 °C for 8 h to remove the CTAB surfactants [12].

Structural analyses were performed by means of X-ray diffraction (XRD: M18XHF-SRC, MAC Science) and small-angle X-ray spectroscopy (SAXS: Nanostar, Bruker) using Cu Kα radiation. Brunauer–Emmett–Teller (BET) surface areas and pore-size distributions were obtained from nitrogen isotherms measured at 77 K with an ASAP 2010 analyzer (Micromeritics). The composition of tin phosphate was characterized by inductively coupled plasma atomic-emission spectroscopy (ICP-AES: ICPS-7500, Shimadzu) and electron-probe microanalysis (EPMA: JXA-8900R, JEOL).

Electrochemical tests were performed with coin-type half-cells (2016 size) using lithium as an anode. The electrode consisted of 60 wt.% active materials, 20 wt.% Super P carbon black, and 20 wt.% polyvinylidene fluoride (PVDF). A mixture of ethylene carbonate/diethylene carbonate (EC/DEC) with 1 M $LiPF_6$ was used as the electrolyte. The cycling tests of the half-cells were carried out between 2.5 and 0.001 V (or between 0.8 and 0.001 V) at a rate of 72 mA g^{-1} (=0.13 C) for the first cycle, and 144 mA g^{-1} afterwards.

3. Results and discussion

The tin phosphates synthesized with various $CTAB/H_3PO_4$ precursor ratios exhibit changes of mesostructures, as shown in Table 1. The d spacings of the mesopores were obtained from the SAXS measurements (Fig. 1(b)), and the average pore sizes were acquired using the Barrett–Joyner–Halenda (BJH) results from the nitrogen-adsorption isotherms. The relative mesopore ratios (in Table 1) were estimated from the measured pore sizes and d spacings of the mesopores (with the assumption of a zero-roughness interface and mono-dispersed mesopores).

The relative mesopore ratios of the tin-phosphate samples are 0, 42, 82 and 100%, respectively. Though the SnF_2/H_3PO_4 precursor ratio was fixed at 1.35, the Sn:P molar ratio of the synthesized powders obtained from the ICP-AES results increases with increasing $CTAB/H_3PO_4$ precursor ratio. In addition, the oxygen contents of the tin phosphates confirmed by the EPMA results are slightly larger than that of $Sn_2P_2O_7$.

The XRD patterns of the as-synthesized tin phosphates are presented in Fig. 1(a). The non-mesoporous (0%) tin phosphate clearly exhibits an orthorhombic β-$Sn_2P_2O_7$ phase [7,15]. (The peak positions were calculated from the atomic positional parameters for β-$Sn_2P_2O_7$ [15] using ATOMS [16].) As the $CTAB/H_3PO_4$ precursor ratio is increased, the mesoporous tin-phosphate samples appear to be amorphous Sn-P-O. In the FT-IR spectra (Fig. 2), the non-mesoporous (0%) tin phosphate exhibits the vibration peaks of the pyrophosphate anion ($P_2O_7^{4-}$) in the spectral region of 500–1300 cm^{-1}. The asymmetric stretching ($\nu^{a}_{PO_3}$) peak of the terminal PO_3 is present at ~1090 cm^{-1}, and the asymmetric (ν^{a}_{POP}) and symmetric (ν^{s}_{POP}) peaks of the P-O-P bridge are clearly visible at ~930 and ~730 cm^{-1}, respectively [6]. The peak at ~550 cm^{-1} corresponds to the bending vibration (δ_{PO_2}) of PO_2 [17]. These peaks remain in the spectra of the tin phosphate with a mesoporous ratio of 42%. As the samples became more mesoporous, however, most peaks except for that corresponding to the PO_3 stretching disappear, which is consistent with the spectra of amorphous phosphates [6] and the X-ray diffraction patterns of Fig. 1. As shown in the SAXS results (Fig. 1(b)), a mesoporous peak is clearly obtained at ~2.25° (d spacing of 4.20 ± 0.63 nm) with an increase in the relative ratio of CTAB to the inorganic precursor. It is supposed that when the over-supplied inorganic precursors are dissolved, part of them

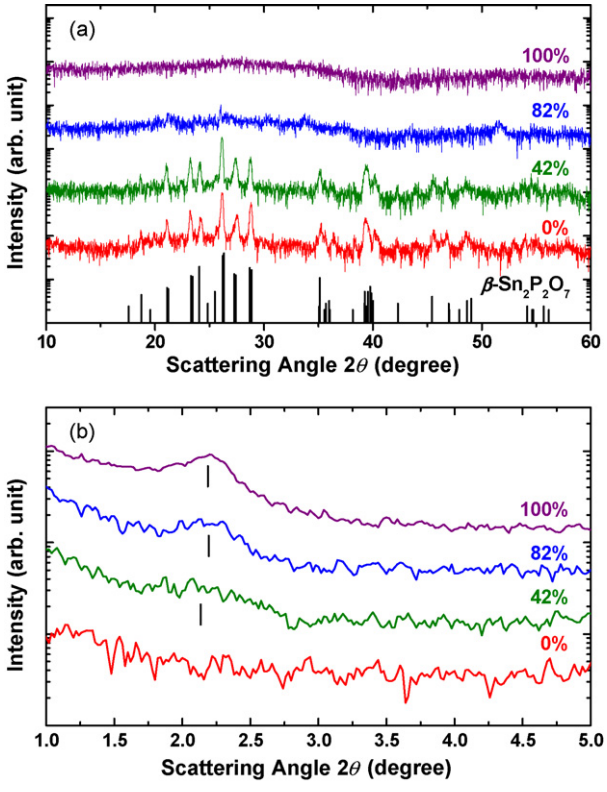

Fig. 1. (a) High-angle and (b) small-angle X-ray diffraction patterns of as-synthesized tin phosphates with various mesopore ratios, using Cu Kα radiation.

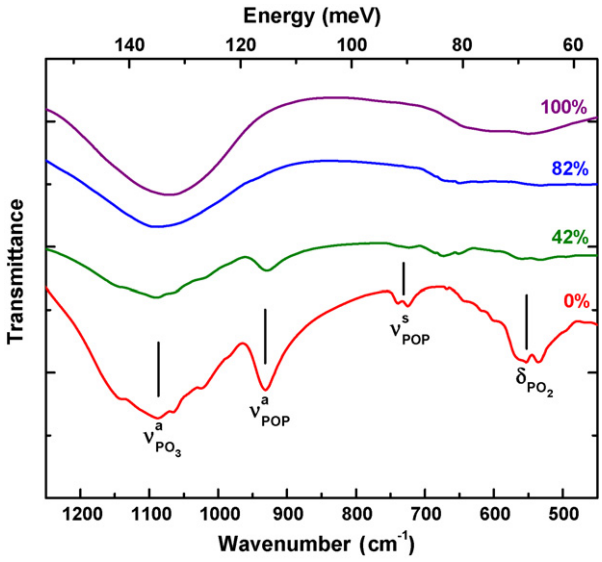

Fig. 2. FT-IR spectra of tin phosphates with various mesopore ratios.

may interact with the CTAB surfactant to form a mesoporous structure. In contrast, the precursors unreacted with CTAB may form non-mesoporous $Sn_2P_2O_7$ particles.

In the nitrogen-adsorption isotherms given in Fig. 3(b–d), the samples have a type IV isotherm [18], which means that they have a mesoporous structure. The BET surface areas of the tin phosphates are 14.7, 114, 167 and 221 $m^2\,g^{-1}$, respectively, (Table 1), and the increase of the surface area correlates with the X-ray diffraction results (Fig. 1). From the nitrogen-adsorption isotherms, the pore-size distributions were obtained using BJH analysis. The average pore size in the annealed samples with mesopore ratios of 42, 82 and 100% is ~2.56, ~2.32 and ~2.33 nm, respectively.

The voltage profiles of the tin-phosphate anodes with the various mesopore ratios are shown in Fig. 4. The non-mesoporous (0%) $Sn_2P_2O_7$ anode delivers an initial discharge capacity of ~780 mAh g^{-1} including the irreversible capacity of ~380 mAh g^{-1} for the lithium-phosphate matrix such as Li_3PO_4 and $LiPO_3$ [6]. Compared with the initial capacities (~400 mAh g^{-1}) and capacity retention (~85% after 5 cycles) of Ref. [6], the non-mesoporous (0%) $Sn_2P_2O_7$ (Fig. 4) has a reasonable initial capacity and capacity retention with a high current rate and a wide voltage range. The plateau at ~1.6 V during discharging may originate from the formation of a lithium-tin-phosphate matrix from the non-mesoporous crystalline tin-phosphate phase. The additional irreversible capacity beyond 260 mAh g^{-1} for four Li^+ ions (in $Sn_2P_2O_7$) may be caused by the formation of a solid-electrolyte-interphase (SEI) layer [19].

As the mesopore ratio is increased, the tin content of the tin-phosphate anodes increases (shown in Table 1) and thus the capacity of the mesoporous tin phosphate is slightly increased. The initial discharge capacity of the tin phosphates with mesopore ratios of 42, 82 and 100% is 880, 1150 and 1220 mAh g^{-1}, respectively. (The capacities of the mesoporous tin phosphates are slightly lower than the values in Ref. [12], probably due to the different Sn-P-O ratios.) The irreversible capacity also increases with increasing mesoporous ratio (~425, ~590 and ~660 mAh g^{-1}, respectively), probably because of the increased formation of an SEI layer due to the large surface area, and the formation of Li_2O from over-supplied oxygen (Table 1). As shown in the insets of Fig. 4, the mesoporous tin-phosphate anode has a peak near 1.1 V (indicated by an arrow) during charge. This may correspond to the re-oxidation of the lithium-phosphate matrix, as in the case of the lithium-oxide matrix in SnO_2 [20,21].

Fig. 5(a) shows the cycle-life performance (charging) of tin phosphates with various mesopore ratios between 2.5 and 0.001 V. As the mesopore ratio increases, the tin content also increases (as shown in Table 1) and thus the capacity

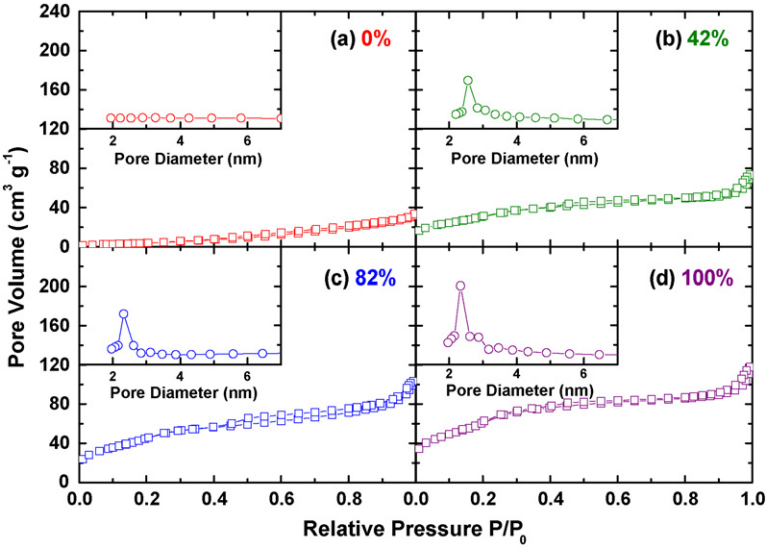

Fig. 3. Nitrogen-adsorption/desorption isotherms of as-synthesized tin phosphates. Insets give pore-size distributions obtained from nitrogen-adsorption isotherms using BJH analysis.

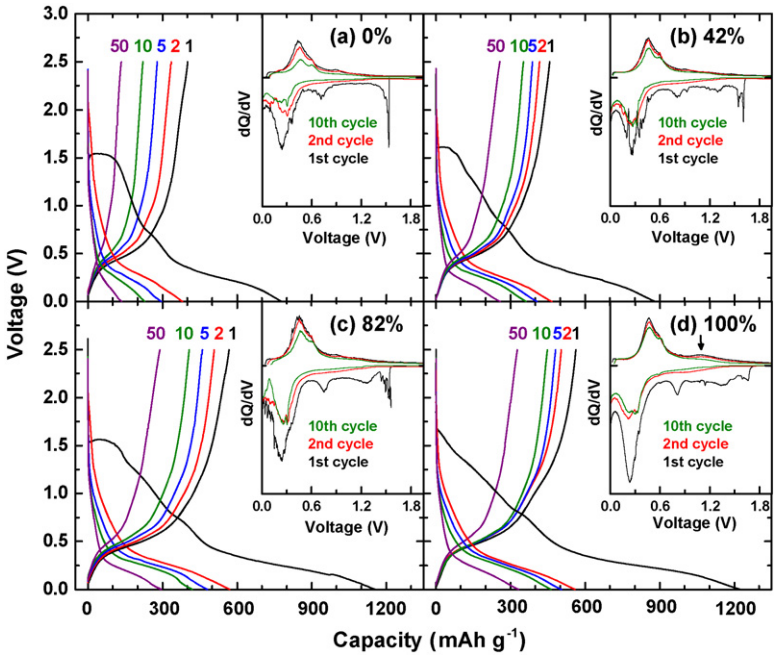

Fig. 4. Voltage profiles of tin-phosphate anodes between 2.5 and 0.001 V. Insets show differential capacities of tin-phosphate anodes (1st, 2nd and 10th cycles).

may become larger. Compared with the charge capacity of ~135 mAh g^{-1} for the non-mesoporous (0%) tin phosphate after 50 cycles (~34% capacity retention of an initial capacity of ~400 mAh g^{-1}), the samples with the mesopore ratios of 42, 82 and 100% exhibit improved capacity retentions of ~56, ~51 and ~58% (~260, ~290 and ~325 mAh g^{-1}), respectively, for initial capacities of ~460, ~570 and ~560 mAh g^{-1}.

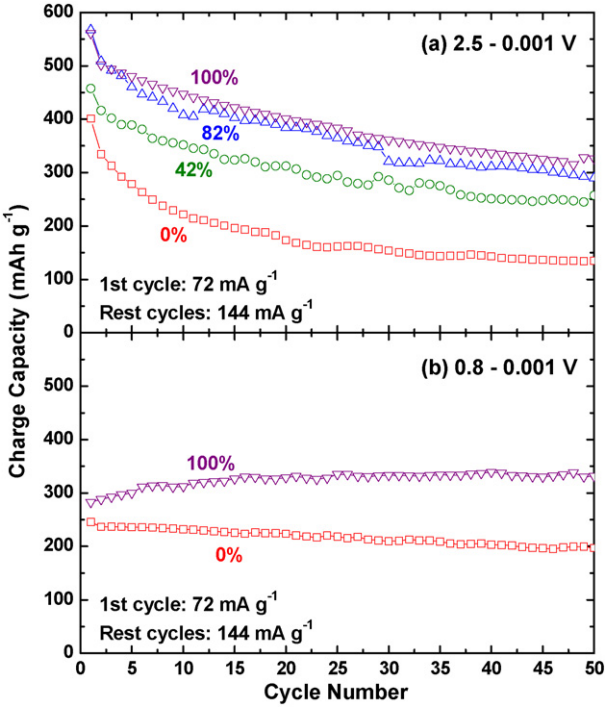

Fig. 5. Cycle-life performance (charging) of tin-phosphate anodes, (a) between 2.5 and 0.001 V and (b) between 0.8 and 0.001 V. First cycle performed at 72 mAh g^{-1} (=0.13 C) and remaining cycles at 144 mAh g^{-1}.

In contrast to the cycle-life performances, the SAXS peaks disappear after 50 cycles between 2.5 and 0.001 V (not shown). Though the mesoporous structures are preserved during the initial few cycles [12,13], the mesoporous characteristic seems to become disordered with increasing cycle number. Deteriorated mesoporous characteristics after 20 cycles have been reported in a previous study [14]. It seems that although the periodic mesoporous structures are destroyed, the contracts between the porous nanostructures remain without breakage. In cycling tests between 0.8 and 0.001 V (Fig. 5(b)), although the capacities decrease due to the limited charge cut-off, the cycling stabilities are greatly enhanced. It may be that the re-oxdiation reaction (~1.1 V peak) of metallic tin with the lithium-phosphate matrix causes deterioration of the mesoporous structures and leads to poorer capacity retention, as in the case of the SnO_2 system [20,21].

4. Conclusions

The mesoporous ratios of the tin phosphates are controlled by adjusting the ratio of surfactant to inorganic precursor. As an anode material for Li-ion batteries in cycling tests between 2.5 and 0.001 V, mesoporous tin-phosphate anodes with mesopore ratios of 42, 82 and 100% exhibit enhanced capacity retention of more than 50%. The corresponding discharge capacities are ~260, ~325 and ~290 mAh g^{-1}, as compared with the ~34% capacity retention (~135 mAh g^{-1}) of the non-mesoporous tin phosphate. The mesoporous structures may alleviate the large volume change that occurs during charge–discharge, even though the mesoporous characteristics are destroyed after 50 cycles. The cycling tests of the 100% mesoporous tin phosphate between 0.8 and 0.001 V exhibit no decay of capacity, which remains at ~325 mAh g^{-1} after 50 cycles.

Acknowledgements

This work was supported by the ERC Program of MOST/KOSEF (R11-2002-102-00000-0), by the Basic Research Program (R01-2004-000-10173-0) of KOSEF, and by the Division of Advanced Batteries in NGE Program (10016446).

References

[1] M.S. Foster, C.E. Crouthamel, S.E. Wood, J. Phys. Chem. 70 (1966) 3042–3045.
[2] C.J. Wen, R.A. Huggins, J. Electrochem. Soc. 128 (1981) 1181–1187.
[3] Y. Idota, A. Matsufuji, Y. Maekawa, T. Miyasaka, Science 276 (1997) 1395–1397.
[4] I.A. Courtey, J.R. Dahn, J. Electrochem. Soc. 144 (1997) 2045–2052.
[5] I.A. Courtey, J.R. Dahn, J. Electrochem. Soc. 144 (1997) 2943–2948.
[6] Y.W. Xiao, J.Y. Lee, A.S. Yu, Z.L. Liu, J. Electrochem. Soc. 146 (1999) 3623–3629.
[7] M. Behm, J.T.S. Irvine, Electrochim. Acta 47 (2002) 1727–1738.
[8] J.S. Beck, J.C. Vartuli, W.J. Roth, M.E. Leonowicz, C.T. Kresge, K.D. Schmitt, C.T.W. Chu, D.H. Olson, E.W. Sheppard, S.B. McCullen, J.B. Higgins, J.L. Schlenker, J. Am. Chem. Soc. 114 (1992) 10834–10843.
[9] S. Schacht, Q. Huo, I.G. Voigt-Martin, G.D. Stucky, F. Schüth, Science 273 (1996) 768–771.
[10] F. Chen, Z. Shi, M. Liu, Chem. Commun. (2000) 2095–2096.
[11] A. Yu, R. Frech, J. Power Sources 104 (2002) 97–100.
[12] E. Kim, D. Son, T.-G. Kim, J. Cho, B. Park, K.-S. Ryu, S.-H. Chang, Angew. Chem. Int. Ed. 43 (2004) 5987–5990.
[13] H. Kim, G.-S. Park, E. Kim, J. Kim, S.-G. Doo, J. Cho, J. Electrochem. Soc. 153 (2006) A1633–A1636.
[14] E. Kim, Y. Kim, M.G. Kim, J. Cho, Electrochem. Solid State Lett. 9 (2006) A156–A159.
[15] V.V. Chernaya, A.S. Mitiaev, P.S. Chizhov, E.V. Dikarev, R.V. Shpanchenko, E.V. Antipov, M.V. Korolenko, P.B. Fabritchnyi, Chem. Mater. 17 (2005) 284–290.
[16] Dowty, ATOMS, Shape Software, Kingsport, Tennessee, 2002.
[17] G.T. Stranford, R.A. Candrate Sr., B.C. Cornilsen, J. Mol. Struct. 73 (1981) 231–234.
[18] S.J. Gregg, K.S.W. Sing, Adsorption, Surface Area, and Porosity, Academic, London, 1982.
[19] M. Wachtler, J.O. Besenhard, M. Winter, J. Power Sources 94 (2001) 189–193.
[20] I. Sandu, T. Brousse, D.M. Schleich, M. Danot, J. Solid State Chem. 179 (2006) 476–485.
[21] M.-Z. Xue, Z.-W. Fu, Electrochem. Solid State Lett. 9 (2006) A468–A470.